OPTIMIZING THE EFFICIENCY OF A RESONANT DIAPHRAGM FLUID DISPLACER

S.D. Percy[1], C.G. Knight[1]
[1]Energy Technology, CSIRO, Newcastle, Australia

Abstract: Diaphragm fluid displacers have application in micro pumps, refrigerators, heat engines and 'lab on chip' technology. However, due to the resonant nature of these devices, in many of these applications the devices are not operating at their maximum efficiency. This paper aims to analyses how different diaphragm and electromagnetic transducer configurations affect the operation and resonant frequency of the fluid displacer, and how the resonant frequency can be detected and controlled to drive the device at its resonant frequency. Six electromagnetic transducer configurations were produced using 3D printing rapid prototyping technology. A purely electronic, voltage-current phase angle detection method to detect the device's resonant frequency has been demonstrated along with a controller that will respond to system changes to ensure the device is operating efficiently. The results show the controller reacting to an environmental change and maintaining the system at resonance. The implementation of this control could increase the efficiency of diaphragm fluid displacers.

Keywords: electromagnetic, diaphragm, pump, resonant, controller, 3D printing, resonance control.

INTRODUCTION

The design of an efficient MEMS actuator and fluid displacer is of interest for use in micro pumps [1], refrigerators [2], [3], heat engines [4] and 'Lab on Chip' technology. Generally, macro-scale implementations of these devices use pistons or rotary turbine pumps to shift the working fluid where required. For a MEMS application pistons and turbines are not practical and instead are often replaced with oscillating diaphragms; these also have the advantages that they require no sealing, no complex extra high tolerance manufacturing, and can be simply produced by MEMS batch processes.

To actuate a MEMS diaphragm the electrical-to-mechanical transducer selected must have a high maximum force, high maximum displacement, and a high maximum frequency to allow for maximum fluid displacement for minimal size. The transducer methods available for this application include piezoelectric, electrostatic, thermal and electromagnetic. Bell et al. [5] presents a comparison between MEMS and macro-scale transducers. In their review, electromagnetic actuators exhibit good displacements, good force and good maximum frequency. They also show that this trait can be transferred between both MEMS and macro transducers. For the experiments outlined in this paper, an electromagnetic transducer using a varying current carrying coil and a permanent magnet will be analyzed.

It is commonly shown that MEMS diaphragm pumps have a resonance, giving a maximum flow rate at one particular frequency. Sandra et al. have designed and tested a MEMS magnetically actuated air micro-pump [6]. In this example the authors used a permanent magnet attached to the top of a silicon diaphragm, which was being driven by an electromagnet. In this article they demonstrated that there was a frequency (5Hz) that allowed maximum flow rate. Additionally, a valve-less electromagnetically-actuated pump has also been designed by Lee et al. in [7]; they demonstrate that the flow rate has a peak frequency (200Hz). In these applications it would be beneficial to be able to easily detect this resonant point, and the maximum flow rate.

The resonant frequency of an electromagnetically actuated oscillating diaphragm is dependent on the inductance of the electromagnetic coil, the weight of the diaphragm, the properties of the fluid it is pumping and the spring co-efficient of the diaphragm (including the air-spring effect of pumping a gas). Analysis of the frequency response of this style of device is far from new; loud speaker designs contain the same components (a permanent magnet, coil, diaphragm and rigid casing). In the case of speaker design the coil resistance and spring coefficient of the diaphragm are selected so that the device's natural frequency of the structure is outside the designed operating frequency of the speaker or human audio range [8]. The result of this is a relatively flat frequency-displacement curve over the designed frequency range. This will mean a high-quality speaker and as a result, will reduce the electrical-to-mechanical (sound) conversion efficiency. In the case of a fluid displacer, maximum displacement velocity for minimum input power is required to provide high efficiency, this means it it is beneficial to drive the device at resonance.

Certain aspects of these devices can change during operation. For example the spring coefficient of the diaphragm can decrease over time due to temperature increases or fatigue, and the air spring due to gas fluid pressure variations. This means it is important to be able to detect that a device is operating at resonance or if a change has occurred that has affected the resonant frequency. It is also important to know how the different transducer configurations affect the displacement and resonance of the device.

The work contained in this article compares the free-air analysis of six small scale diaphragm-actuator configurations. The six configurations have been designed in 3D CAD and printed on a rapid prototyping 3D printer. The evaluation will compare the peak displacement, input power for a fixed voltage, the device's resonant frequency and the phase difference between voltage and current. The use of rapid prototyping allows the devices to be produced and tested very quickly. The analysis will aim to remain relevant when scaled. The final section demonstrates a purely electronic, voltage-current phase angle method to detect the device is operating at its resonant frequency. Finally a PID controller has been implemented on one of the prototypes which will adaptively determine the resonant frequency without needing to know the diaphragm displacement.

METHOD

Six devices with differing actuator configurations have been designed in 3D CAD and produced on an Objet Alaris 3D printer. Each device contains a 40mm diameter, 0.13mm thick diaphragm, electromagnetic actuator and a solid body to encase the components. The configuration has been designed to allow two diaphragms to be actuated back-to-back. This allows the driving signals to each of the two actuators to be supplied in series to double the fluid displacement, or be supplied independently to allow a phase shift between the two diaphragms; this would be useful in the operation of a heat engine or refrigerator.

Fig. 1 shows the three designs, and two variations of each. The first design, AC1, uses a large magnet between two flat coils attached to the diaphragm, with the coils spaced from the magnet by 1.5 mm to allow forward and backward actuation. A disadvantage of this design is that the diaphragm will not achieve constant force; the peak force applied to the diaphragm will be when the coil moves closest to the centre magnet. The advantage of this design is that a large magnetic field can be achieved using the large rare earth magnet. There are two versions of this device: AC1.1 using a small coil and AC1.2 using a larger coil.

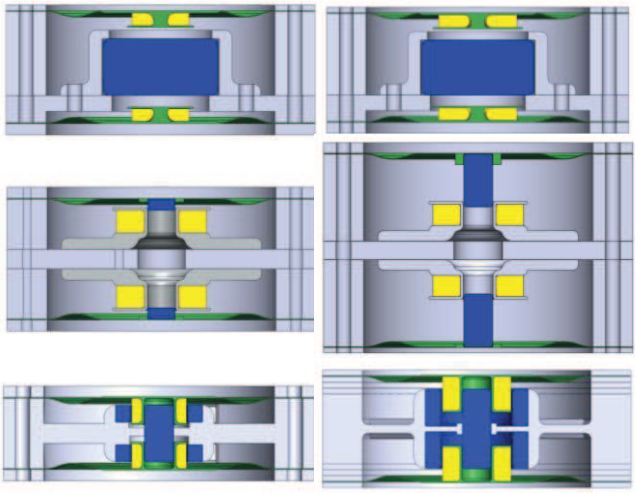

Neodymium permanent magnets, *Copper coils,* *Diaphragms*

Fig. 1: Six test devices: Top - AC1 (large centre magnet with flat coils attached to the diaphragms). Middle - AC2 (small and large magnet attached to the diaphragm with a large stationary coil). Bottom - AC3 (doughnut and cylindrical centre magnetic pole, coil attached to the diaphragm).

The AC2 device uses a coil with a high number of turns attached to the solid casing and a small cylindrical rare earth magnet attached to the diaphragm with the north pole entering the coil. The advantage of this design over AC1 is that the maximum force is achieved at the neutral position of the magnet, and will remain relatively constant over small displacements; also a high magnetic field can be achieved using the larger coil and allowing for a higher power handling capacity. AC2.2 uses a larger magnet than AC2.1, which results in a larger magnetic field and a larger diaphragm mass. This is very similar to the MEMS actuators used in [6][7], being a permanent magnet attached to the diaphragm and a coil mounted close to the diaphragm.

The final design, AC3, implements two back-to-back actuators in a similar configuration to that used in a voice-coil loud speaker [8]. This coil is designed to overhang the magnetic field, resulting in a portion of the coil always being in the magnetic field; this causes a constant force-displacement relation for small displacements. AC3.1 has a smaller magnet and a smaller coil than AC3.2. The larger coil will allow more power to be applied to the actuator and result in a larger displacement.

The power handling capacity of each device is limited by the number of coils and the thermo-mechanical properties of the 3D printer's VeroWhite Plus material [9]. The mechanical properties of the material changes as the temperature of the material

varies between the glass transition temperature 53°C [9] and the material decomposition temperature of 300°C. The ability to keep the coil away from the diaphragm or to dissipate heat will increase the power handling capacity.

EXPERIMENTAL PROCEDURE

To evaluate the six diaphragm actuators, the experimental setup in Fig. 2 was used. The experiment used a dSPACE RTI1104 system (real time rapid prototyping hardware) to produce a sinusoidal test signal which was amplified using a power amplifier to drive the device under test. A displacement laser measured the position of the actuator. The data acquisition of dSPACE was used to log the AC supply voltage, current and displacement of the device under test.

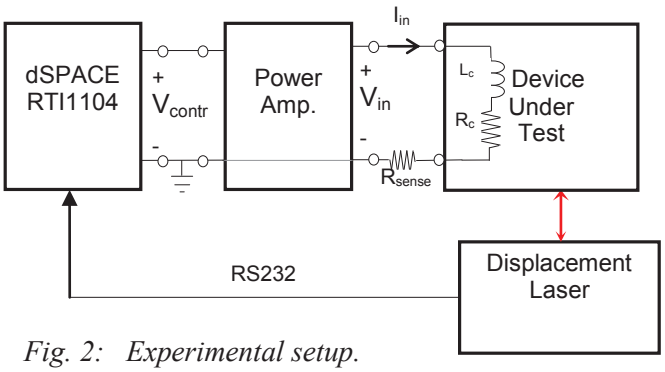

Fig. 2: Experimental setup.

To form a frequency sweep of each device, the control signal (V_{contr}) supplied from dSPACE was programmed to increment in frequency by 0.5Hz every 3-seconds, from 20Hz to 500Hz. As each device has a different coil resistance the amplitude of V_{contr} was adjusted to supply 500mA to the test actuators for a supply frequency of 20Hz, the power amplifier will maintain a constant voltage across the test device throughout the frequency sweep. This allowed a comparison between the current-carrying capabilities of each actuator and the actuator's displacement amplitude.

In post-processing of the measurements, the voltage and current were split up into 2-second segments, neglecting the first 1 second of each frequency test as 'settling time'. The power phase angle between voltage and current was found by taking a Fast Fourier Transform of each and determining the phase angle (ϕ) of the most significant frequency component; this has been implemented in [10]. The RMS voltage and current for each 2-second segment were determined and $|P| = V_{rms} I_{rms} cos\phi$ was used to give the magnitude of active power doing work to displace the diaphragm.

This experiment allows the six actuators to be evaluated for the level of electrical power the device could handle for the initial supply current of 500mA, the peak displacement, the frequency of resonance and the ability to detect resonance of the device.

Fig. 3, shows the detection phase angle and the corresponding input power and displacement achieved verse frequency for each of the six devices. It will be noticed that when the device begins to resonate, input power reduces (due to the constant voltage applied) and displacement increases very significantly. This demonstrates the greatly improved efficiency at this frequency.

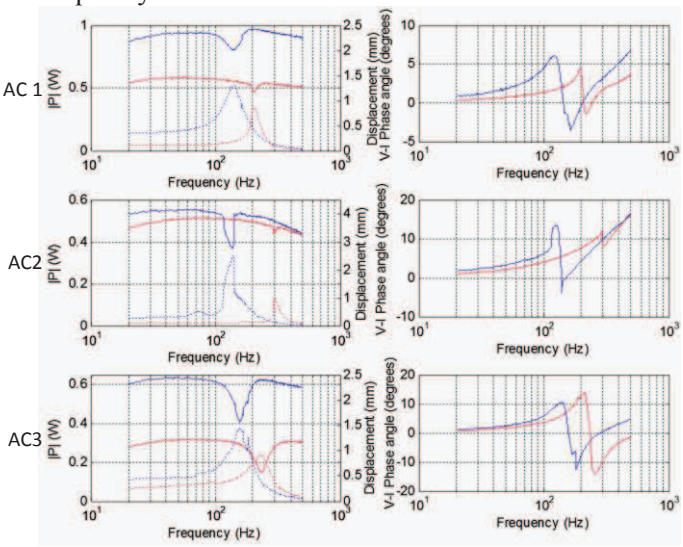

Fig. 3: Comparison between actuator configurations, Red indicates ACx.1 and blue indicated ACx.2. Left, Solid lines indicates |P| and dashed lines indicate displacement.

Shown on the right column in Fig. 3 is the phase angle of each device. In each graph, as the device hits resonance, there is a phase shift between voltage and current. This demonstrates that the phase shift can be used to detect if the device is operating at its resonant frequency. The requirements for this sensing to operate are purely electronic requiring only a measure of the supply voltage and current using a current sense device (Hall Effect or sense resistor), and electronics to detect the phase angle between the two.

Using the resonant sense method discussed, a PID controller was implemented in dSPACE for AC3.1 (the red curves from the bottom graphs) to control the supply signal frequency and maintain the voltage-current phase angle that occurs when the device is at resonance. For this device the voltage-current phase angle of resonance was 0 degrees. To demonstrate this controller working a change in fluid pressure was introduced by sealing the free-air port in order to

observe the controller reacting to a system change.

RESULTS

Fig. 3 shows the controller reacting to an introduced change in fluid pressure that occurs by sealing the free-air port on the device. At startup, in the 'free air condition' (that is, with the vent ports open), the controller increases its operating frequency to detect the device resonance when the phase angle between voltage and current equals 0 degrees. Resonance is detected at 220Hz (matching to the measured resonance from Fig. 3); as a result the displacement increases and supplied power decreases. As indicated at approximately 8s the device's air port is sealed, increasing the resonant frequency of the device. This causes the phase angle between voltage and current to instantly change; as a result the device draws more electrical power and the displacement decreases. To deal with this the controller increases the supply signal frequency up to the new resonant frequency of 340Hz, resulting in a voltage-current phase angle of zero degrees. Once the resonant frequency is detected the electrical power reduces and displacement increases. The increased pressure with the free-air port sealed means that the displacement has a lower value than at start up. For demonstration purposes the control parameters selected result in a relatively slow response to a change, tuning these would increase this.

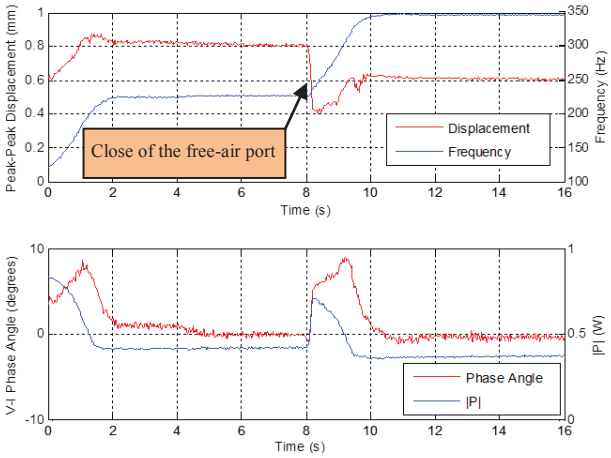

Fig. 4: Results showing the controller detecting the device's resonant frequency and reacting to a system change.

CONCLUSION

The results showed how different electromagnetic configurations affect the fluid displacer frequency and ability to detect resonance. The analysis has outlined how the device's resonant frequency can be detected using a purely electronic method (with no need for a displacement sensor). The final result demonstrated a controller that will adjust the operating frequency to the device resonance using the sensing method.

The implementation of a system using this methodology will allow higher efficiency MEMS fluid displacers. This will potentially allow for the increased uptake of micro-pumps, micro-refrigerators, heat engines, 'Lab on Chip' technology and more.

REFERENCES

[1] H. Chang, C. Lee, C.Y. Wen, and B.-S. Hong, "Theoretical analysis and optimization of electromagnetic actuation in a valveless microimpedance pump," *Microelectronics Journal*, vol. 38, no. 6–7, pp. 791–799, Jun. 2007.

[2] P. P. P. M. Lerou, G. C. F. Venhorst, C. F. Berends, T. T. Veenstra, M. Blom, J. F. Burger, H. J. M. T. Brake, and H. Rogalla, "Fabrication of a micro cryogenic cold stage using MEMS-technology," *Journal of Micromechanics and Microengineering*, vol. 16, no. 10, pp. 1919–1925, Oct. 2006.

[3] C. Tsai, R. Chen, C.L. Chen, and J. DeNatale, "Micromachined stack component for miniature thermoacoustic refrigerator," *Micro Electro Mechanical Systems, 2002. The Fifteenth IEEE International Conference on*. pp. 149–151, 2002.

[4] W. P. Huesgen Till, "Design and analysis of a novel MEMS-heat engine for power generation," pp. 96–99, 2009.

[5] D. J. Bell, T. J. Lu, N. a Fleck, and S. M. Spearing, "MEMS actuators and sensors: observations on their performance and selection for purpose," *Journal of Micromechanics and Microengineering*, vol. 15, no. 7, pp. S153–S164, Jul. 2005.

[6] S. Santra, P. Holloway, and C. D. Batich, "Fabrication and testing of a magnetically actuated micropump," *Sensors and Actuators B: Chemical*, vol. 87, no. 2, pp. 358–364, Dec. 2002.

[7] C.Y. Lee, H.T. Chang, and C.Y. Wen, "A MEMS-based valveless impedance pump utilizing electromagnetic actuation," *Journal of Micromechanics and Microengineering*, vol. 18, no. 3, p. 035044, Mar. 2008.

[8] K. Thorborg, A. D. Unruh, and C. J. Struck, "An Improved Electrical Equivalent Circuit Model for Dynamic Moving Coil Transducers," pp. 1–13, 2007.

[9] Objet, "Materials Data Sheets Materials Simulating Engineering Plastics," *Materials Data Sheet*, 2010.

[10] S. Sawant, "Find phase difference between two sinusoidal signals," 2010. [Online]. Available: http://www.mathworks.com/matlabcentral/fileexchange/29075-find-phase-difference-between-2-sinusoidal-signals. [Accessed: 10-May-2012].